Effects of Sedimentologic and Stratigraphic Heterogeneity on Production in Carbonate Reservoirs: An Integrated Outcrop, Synthetic Geologic Modeling, and Flow Simulation Study

By

Steven Randall Herbst

Submitted to the graduate degree program in Geology
and the Graduate Faculty of the University of Kansas
in partial fulfillment of the requirements for
the degree of Master of Science.

_____

Chair: Dr. Eugene Rankey

_____

Dr. Stephen Hasiotis

_____

Dr. Reza Barati

Date Defended: 02/02/16

The Thesis Committee for Steven Randall Herbst
certifies that this is the approved version of the following thesis:

Effects of Sedimentologic and Stratigraphic Heterogeneity on Production in Carbonate Reservoirs: An Integrated Outcrop, Synthetic Geologic Modeling, and Flow Simulation Study

_____

Chair: Dr. Eugene Rankey

_____

Dr. Stephen Hasiotis

_____

Dr. Reza Barati

Date approved: 2/16/2017

ABSTRACT

Most geoscientists recognize, characterize, and understand the many scales and types of heterogeneity in carbonate reservoirs; however, systematic quantitative assessment of the impact of this range of geological variations on production from carbonate reservoirs is rare. To explore and quantify the impact of geologic heterogeneity of hydrocarbon production from carbonate shoreface reservoirs, this study couples an outcrop-derived conceptual model and petrophysical data from reservoir analogs to generate a spectrum of simple geologic models of carbonate shoreface reservoir systems. The 25 geologic models, designed to isolate and evaluate the influence of geologic variables, capture a range of heterogeneity related to depositional geometry, facies stacking patterns, diagenetic surfaces and bodies, porosity distribution, and permeability distribution. A total of 750 flow simulations of these geologic models provide a means to quantify the impact, relative importance, and risk associated with each geologic factor on original oil in place (OOIP), production rate, and cumulative production.

Results reveal how geological parameters influence OOIP and dynamic production measures. For example, in the absence of flow baffles (subaerial exposure surfaces or flooding units), the presence of clinoformal geometries does not markedly influence static or dynamic production metrics. In contrast, the presence of flow barriers along clinoform surfaces can result in marked (in excess of 30%) changes in production, accompanied by minimal change in OOIP. Changing either facies proportions (e.g. foreshore:upper shoreface:lower shoreface) or porosity (mean porosity) impacts both static and dynamic reservoir attributes, in many cases by more than 10% from the base model. Collectively, these results, derived from systematic analysis of a suite of simple (but fully constrained) models, quantify the impacts and risks associated with a range of geological parameters. These insights can be used to characterize, understand, and

predict the important roles and risks of geological variability on production of comparable subsurface reservoirs.

ACKNOWLEDGEMENTS

Funding for this project was provided by the Kansas Interdisciplinary Carbonate Consortium (KICC) and software (Petrel and Eclipse) was provided by Schlumberger.

I am profoundly grateful to everyone at the Department of Geology at the University of Kansas who made the past few years a wonderful experience. First, and foremost, I acknowledge my advisor, Dr. Rankey, for giving me this opportunity. I am eternally grateful for his advice, support, patience, and guidance. I am also grateful for my committee members, Dr. Hasiotis and Dr. Barati, for their time and assistance throughout the writing process. A special thanks to Dr. Barati for his efforts with Petrel. Similarly, I would also like to thank Dr. Hassan Eltom for assisting me during the beginning stages of learning Petrel.

Thanks to the Bahamian government for the research permit. I am especially grateful to Dennis Thompson and Robbie Gibson, our Bahamian boat captains, whose expertise permitted safe and enjoyable during our daily trips to our outcrop locations. I would also like to thank the Crooked Island Lodge staff and the people of Crooked Island for their hospitality. I am extremely grateful for Alexa Goers and the assistance she provided in the field and throughout the completion of this work. Abdul Wahab and Maritha Huber also provided valuable assistance while in the field.

Finally, I would like to thank my friends and family for the support and strength they provided throughout the duration of my time at the University of Kansas.

TABLE OF CONTENTS

LIST OF FIGURES AND TABLES

FIGURES

TABLES

INTRODUCTION

Carbonate reservoirs are notoriously heterogeneous, at scales ranging from the pore throats to depositional sequences (Kjonsvik et al., 1994; Palermo et al., 2010). Evaluating, predicting, and exploiting hydrocarbon resources in carbonate reservoirs commonly utilizes reservoir modeling and flow simulation, yet the range of complex depositional (Kjonsvik et al., 1994; Shekhar et al., 2014) and diagenetic (Shekhar et al., 2014) heterogeneities complicates predictive reservoir modeling. The variability in these systems are controlled by a range of depositional and diagenetic factors, the influences of which make accurate predictions of production characteristics (e.g., original oil in place [OOIP], production rate, cumulative production) challenging (Fitch et al., 2014; Shekhar et al., 2014).

To gain insight into the nature, scale, and controls on heterogeneity, subsurface data and outcrop analog studies are common sources of quantitative data for reservoir modeling (e.g., Palermo et al., 2010; Eltom et al., 2012; Jung and Aigner, 2012; Amour et al., 2013; Lipinski et al., 2013). Borehole-derived data (e.g., log suites and core) from reservoirs can provide a preview of < 1% of the actual reservoir (Lucia, 2007), and only capture the details of geologic variability of one location. On the other hand, seismic surveys can reveal the three-dimensional (3D) reservoir architecture, but at a relatively coarse scale. To garner additional insight, outcrop analogs that provide for potentially continuous 3D observations at multiple scales (Palermo et al., 2010; Tomas et al., 2010; Amour et al., 2013) can be used to test the quality of stochastic models (MacDonald and Assen, 1994) or reduce uncertainty regarding the analogous reservoir (Eltom et al., 2012). Outcrops, however, are limited because they represent one unique, distinct geologic realization, and include features or reservoir characteristics that may or may not reflect heterogeneities present in the reservoir of interest.

An important role of a reservoir model is to provide a geologically realistic framework to assess the complexity of the reservoir for visualization and simulation, because the majority of the reservoir cannot be observed and characterized (e.g., Lucia, 2007; Shekhar et al., 2014). Modeling efforts rely heavily on algorithm-based stochastic methods and are shaped by the prior experience and training of a geologist (e.g., Deutch, 2002; Amour et al., 2012). Kerans and Tinker (1997) suggest that 3D geologic models are built first in the mind, based on outcrop and core data. This process, however, commonly leads to a myriad of questions or assumptions concerning the possible influences of geological parameters interpreted to be important in controlling production from the reservoir.

In this context, this study ***systematically explores and quantifies the role and relative importance of geologic variability (e.g., stratigraphic geometry, connectivity within and between successions, and porosity and permeability distribution) on hydrocarbon production from carbonate systems*** through analysis of a suite of *what if?* scenarios (Agar and Hampson, 2014). This paper uses a range of geologically plausible scenarios represented by simple, idealized synthetic reservoir models of carbonate shoreface systems in which variables are systematically isolated and evaluated, while holding all engineering parameters constant. These models are inspired by (and based broadly on) the outcrop character of well-exposed, Pleistocene–Holocene, margin-parallel, oolitic-skeletal shoreface systems of Crooked Island and Long Cay, southern Bahamas. As the focus is not on modeling any one particular reservoir, this study has the luxury of exploring a full range of geological parameters and scenarios, the results of which illustrate and quantify the relative importance of those parameters on production from carbonate shoreface successions.

CONCEPTUAL GEOLOGIC FRAMEWORK FOR MODELING

The sedimentology, facies, and depositional geometries of Pleistocene successions on Crooked-Acklins Platform (CAP), an isolated carbonate platform in the southeastern Bahamas (Figure 1), provide a realistic framework of geologic heterogeneity for the construction of geologic models of carbonate shoreface systems. Numerous studies have described facies variability of comparable well-exposed Pleistocene–Holocene shallow marine deposits in the Bahamas and the nearby Caicos Platform (e.g., Inden and Moore, 1983; Lloyd et al., 1987; Strasser and Davaud, 1986; Hearty and Kindler, 1993, 1997; Aalto and Dill, 1995; Aurell et al., 1995; Carew and Mylroie, 1995; Wanless and Dravis, 2008; Rankey, 2014).

CAP includes three major islands: Crooked Island in the northwest, Acklins Island in the east, and Long Cay in the southwest. On the western flanks of Crooked Island and Long Cay, sea cliffs (up to 6 m high) expose the Pleistocene succession for several km (along and across depositional strike), and in this area is a broadly analogous active oolitic shoreface (Strasser and Davaud, 1986; Rankey, 2014). Examining these geologically young strata provides constraints because both modern and ancient systems can be examined and directly related, and in many cases, plan-view geometries are exposed. A more complete description will be provided in the Master's thesis of Alexa Goers, later in 2016.

Akin to the Holocene succession (Rankey 2014), a typical succession from Long Cay consists of a number of distinct facies (Figure 2, Table 1). In several locations, the base of the succession includes Facies A, a coral-dominated framestone to boundstone composed of *in situ* corals (e.g., *Acropora cervicornis, Diploria*, *Montastrea*, *Porites*) and coral rubble (primarily *Acropora cervicornis)* in a skeletal grainstone matrix. These deposits are discontinuous along

strike, but can extend over 0.5 km. Facies A is interpreted to represent deposits of reefs. The reef facies is not represented in models.

This unit is overlain by a grainstone succession. Extensively bioturbated grainstone is locally present (Facies B, Table 1) at the base of the section. Commonly, however, Facies A is overlain by Facies C (Table 1) an ooid-peloid-skeletal grainstone with an open marine fauna, including *Halimeda*, mollusks, and foraminifera. This unit is moderately well sorted, medium to coarse sand, and trough cross laminated. These strata commonly are overlain by Facies D (Table 1), a distinct grainstone that includes low-angle (2–11º), seaward-dipping planar laminations, alternating coarse–fine laminations, and keystone vugs (fenestrae). The succession in many areas is capped by Facies E, an undulatory, relatively continuous unit (up to 1 m thick) that includes rhizoliths (casts, molds, and tubules), laminated crusts, and karst features (dissolution pits, collapse breccia).

These facies typically occur in a systematic succession. On the basis of sedimentary structures, biota, and their succession, and by comparison with nearby modern analogs (Rankey 2014), are interpreted to represent deposition in environments from reef (Facies A), lower shoreface (Facies B), upper shoreface (Facies C) and foreshore (Facies D), and capped by a subaerial exposure surface or intensely altered zone (Facies E) (Table 1).

High-resolution satellite imagery of the area (Figure 3) shows a plan-view surface pattern of broadly margin-parallel, elongate topographic ridges. These topographic ridges correspond to the shoaling upward shoreface successions along the coast (cf. Figure 2). Collectively, the succession is interpreted to represent a series of prograding shorefaces, which, on the basis of superposition and cross-cutting relationships, can be grouped into ridge sets that prograde west (Figure 3C). The data reveal more than 1 km of ridge set progradation at the southern end of

Long Cay and almost 2 km at the southern end of Crooked Island. The absolute ages of these ridges are unknown (cf. Hearty and Kindler, 1993), but for the purposes here, these ages are not relevant.

As these Pleistocene shoreface strata are young and have not been buried, their porosity and permeability generally are not informative for modeling reservoirs. Instead of using data from the Pleistocene succession, the geologic models described below capture the range of petrophysical variability in subsurface oolitic reservoirs, including the Jurassic Smackover of the Gulf coast (Moore, 1997; Handford and Baria, 2007), the Jurassic Dogger of the Paris basin in France (Cussey and Friedman, 1977), and the Lansing-Kansas City groups in Kansas (e.g., Watney and French, 1988). These reservoirs exhibit a broad spectrum of porosity and permeability (Figure 4); their ranges and absolute minimum and maximum values provide bounds for porosity and permeability in geologic models. For this study, the specific rock properties assigned to facies simply are taken to be the net result of original depositional and subsequent diagenetic overprinting (e.g., Yose et al., 2006; Shekhar et al., 2014).

GEOLOGIC MODELING

The geologic foundation from outcrops and reservoir analogs provide a framework for building the suite of simple, idealized geologic models. This suite of models attempts to capture the essence of the influence of geological parameters and develops broadly applicable understanding, without trying to reproduce one specific reservoir or outcrop analog. As such, the geologic models capture the range of variability of possible geologic heterogeneities. These heterogeneities are divided into three groups: 1) facies and stratigraphic geometry (e.g., clinoforms versus layer-cake geometries; variable facies-stacking patterns and stochastically distributed properties), 2) diagenesis, which impacts connectivity between ridge sets (e.g.,

presence or absence of permeability barriers or conduits, and different properties among ridge sets), and 3) distribution of porosity and permeability within and among stratigraphic units. As all of these geological variables use a variety of realistic geological values, the models simulate a spectrum of geologically plausible scenarios that could exist in subsurface reservoirs.

METHODS

Modeling Framework

A suite of 25 geologic models, built in Petrel, reflect different aspects of the conceptual model of carbonate shoreface deposits, and explicitly include several scales of potentially influential geologic heterogeneities. Construction of facies models included several major iterative steps. The first step is creating a relatively deterministic framework, based on 36 facies-based pseudo-logs and predetermined surfaces. The second step is defining zones. Most models use three shingled clinoformal zones, constrained by surface inputs, mimicking three progradational ridge sets. Layering for clinoform-based models follows the base or top surface for each zone to honor the internal stratigraphic architecture of clinoform geometries. In addition to these clinoform models, other contrasting facies models are layer-cake with parallel horizontal layers.

The resultant model framework dimensions measured 2 km long x 2 km wide x 20 m thick. Models with cell dimensions (I, J, K) of 20 m x 20 m x 1 m (578,136 cells) qualitatively illustrate geologic heterogeneity. Flow simulations used a coarser grid with 50 m x 50 m x 1 m (94,248 cells) cell dimensions.

Stochastic population of interwell facies utilized Truncated Gaussian Simulation (TGSim), chosen to honor the systematic shallowing-upward facies patterns of shoreface systems (Amour et al., 2013; Cao et al., 2014). These facies models are comprised of three facies (from

base to top): lower shoreface, upper shoreface, and foreshore. In some models, zones 0.5 m thick with distinct petrophysical properties (either exceptionally low or high) along clinoform surfaces mimic the possible presence of subaerial exposure surfaces (i.e., Facies E). Prior to populating models with continuous properties (porosity and permeability), facies models were averaged using arithmetic mean calculations from 30 realizations. These multiple realizations act to reduce uncertainty related to synthetic conditioning data (the psuedo-wells), stochastic aspects of facies distribution, and the choice of algorithm for interwell property distribution (Falivene, 2006; Amour et al., 2012).

During model construction, multiple aspects of the petroleum system were simply assigned to the models, but could be variable as well. For example, the trapping mechanism is a stratigraphic pinch-out landward with impermeable layers (i.e., seals) above and below the reservoir. These impermeable bounding units were not explicitly modeled to minimize the total number of cells for simulation purposes and because Petrel assigns impermeable boundaries to undefined cells. Similarly, to focus on stratigraphic influences on heterogeneity, the models did not include faults or fractures, although these features can be important in some reservoirs (e.g., Yose et al., 2001; Agar et al., 2009). Finally, the reservoir was placed at 1400 m depth to mimic reservoir depths similar to the Lansing-Kansas City reservoirs in Kansas (Watney and French, 1988).

Modeling Geologic Heterogeneities

This study models several scales of potentially influential geologic heterogeneities: 1) depositional geometry, 2) stratal architecture, and 3) petrophysical property variance (Figure 5; Table 2, 3). The various scenarios are derived from combinations of these heterogeneities, and in results are reported relative to a base case.

Depositional geometry

Depositional geometries for the majority of the facies models used low-angle clinoforms that simulate prograding ridge sets (Handford and Baria, 2007). Clinoform dimensions are 1 km long, 20 m high, and 1º inclined, and are laterally offset (with no topset aggradation; mimicking the outcrops). Within designated reservoir units, layering honors the inclined clinoform geometry, with an average layer thickness of 1 m. Other models used simple layer-cake geometry.

Facies architecture

Facies distribution was modeled using the TGSim algorithm because of the ordered shallowing-upward trend in shoreface facies associations (MacDonald & Aasen, 1994; Deutch, 2002; Handford and Baria, 2007; Rankey 2014; Figure 2, 5). From base to top, the three facies throughout the models include lower shoreface, upper shoreface, and foreshore. Facies proportions are represented in the modeling nomenclature as a three-digit ratio for the relative vertical distribution of the three reservoir facies (in order, foreshore:upper shoreface:lower shoreface). The majority of models, including the base model use a facies proportion of 1:1:3, whereas selected models use facies proportions of 1:2:2 and 1:3:1.

Select models exhibit a purely stochastic facies distribution using sequential Gaussian simulation (SGS). These models evaluate the general absence of geologic constraints. Facies proportions for these models are the same as the base model.

Diagenetic surfaces and bodies

Subaerial exposure surfaces are common in Pleistocene and older carbonate strata. These subaerial exposure surfaces represent periods of possible meteoric diagenesis during relative falls

and lows of sea level, and can separate prograding highstand shoreface deposits (i.e. ridge sets) (Carew and Mylroie, 1995). As they are diagenetic interfaces, subaerial exposure surfaces can markedly influence porosity and permeability (e.g., Esteban and Klappa, 1983; Goldhammer and Elmore, 1984; Goldstein 1988; Dickson and Saller, 1995). They commonly are modeled as clinoform-bounding surfaces, and can form permeability barriers that have a profound impact on reservoir connectivity and fluid flow (e.g., Arakel, 1982). Diagenetic modifications related to subaerial exposure, however, can either enhance or reduce porosity and permeability (Dickson and Saller, 1995; Moore, 1997; Yose et al., 2006).

To explore the possible role of diagenetic surfaces on production, the depositional facies architecture for several models was modified to include a subaerial exposure surface. This surface was introduced between clinoforms. Although these surfaces and zone of intense alteration are commonly undulatory and laterally vary in thickness (as observed on Long Cay), the surface was simplified and modeled as a one cell-thick (0.5 m) zone. During the modeling process, exposure surfaces were designated as separate zones to better control reservoir properties and to determine whether they enhance (conduit) or inhibit (barrier) fluid flow and connectivity between ridge sets.

In other scenarios, subaerial exposure alters not just one thin zone, but instead it modifies an entire succession, with strata above (or below) exhibiting a different diagenetic history. To simulate these plausible scenarios, two models included individual clinoforms (bound by surfaces) with porosity that was either higher (mimicking dissolution) or lower (mimicking cementation) than the other clinoforms. As such, these clinoforms represent diagenetically modified stratigraphic bodies.

Petrophysical variability

Distribution of reservoir petrophysical parameters commonly is controlled by facies; therefore, the models use a facies-based distribution of continuous properties (i.e., porosity and permeability) (e.g., Sahin et al., 1998; Eltom et al., 2012) (Figure 5). Cells were populated with synthetic porosity and permeability values derived from analog reservoir values (Table 3) using sequential Gaussian simulation (SGS). Porosity distribution used a normal distribution, whereas permeability had a log-normal distribution, and, in Petrel, input parameters are simplified to mean and standard deviation values (Figure 5, Table 3). Values and ranges of analog reservoir petrophysical parameters are conditioned to the respective facies model. Several models used purely stochastic (not facies-based) property population. Note that inherent uncertainty related to facies modeling introduces additional uncertainty to porosity and permeability models (Eltom et al., 2012).

Flow Simulations and Uncertainty

A common method for evaluating and quantifying the efficiency of geologic models is to take them through reservoir flow simulations (e.g., Kjonsvik et al., 1994; Carrasco et al., 2001; Jackson et al., 2009; Fitch et al., 2014; Shekhar et al., 2014). Flow simulations enhance understanding and allow quantification of the role and relative impact of static geologic heterogeneities impact production on the dynamic behavior of fluid flow (Carrasco et al., 2001).

This study evaluates the relative impact of heterogeneities from the series of geologic models using OOIP (static), production rates and cumulative production (dynamic) as metrics. Since this project is not simulating a particular reservoir or outcrop analog, engineering parameters are held constant to isolate the role of geologic variability on production. Twenty five modeled geologic scenarios were each taken through a set of 30 primary-recovery reservoir

flow simulations in ECLIPSE using an Eclipse 100 black oil model, for a total of 750 simulations.

To explicitly evaluate the effect of heterogeneity on production response, cell sizes were kept relatively small to capture as much detail of the modeled heterogeneity as possible. To assess efficiency and practicality of cell dimensions for flow simulations, sensitivity modeling was performed on an initial model using 9 grid variations using a combination of cell dimensions (I and J) of 10m, 20m, and 50m and layering (K) of 0.25m, 0.5m and 1m. Flow simulations for 10m and 20m cell dimensions (I and J) failed to produce efficient, repeatable results due to CPU limitations, therefore cell dimensions of 50m x 50m x 1m were used for simulation grids. To accommodate for the lack of upscaling, relatively small cell size, and total number of simulations (750), simulations were limited to one year for CPU and time efficiency. One-year simulations exhibited the same trend as the few successful longer-term simulations.

To accomplish simplified and idealized flow simulations, Petrel defaults for reservoir and fluid properties were used and kept constant for all models (Table 4). One simulated vertical production well in the center of the model used a simple completion that was cased and perforated over the entire reservoir interval. Further simplification was attempted by placing the gas-oil contact and oil-water contact 25 m above and below, respectively, the reservoir interval. Simulations used a net-to-gross ratio of 1.

Uncertainty is introduced throughout the modeling process (Eltom et al., 2012). Variability among stochastic model realizations is just one source of uncertainty. Given that each stochastic model has tens of thousands statistically equiprobable realizations, each of which honor input parameters, 30 realizations of the same property model were used to evaluate and

quantify the inherent uncertainty related to the petrophysical modeling process and flow simulations (King and Mansfield, 1997; Lui et al., 2001; Deng et al., 2011).

Results from the 30 simulations were used to calculate measures for comparative analysis of OOIP, cumulative production after one year, and production rate on the last day of the first year of production. These analysis metrics are described as several values: minimum, p10 (pessimistic), p50 (median), average, p90 (optimistic), and maximum values (Sykes et al., 2012). These measures are used to rank the role and relative importance of modeled heterogeneities.

GEOLOGIC MODELING AND SIMULATION RESULTS

The suite of 25 geologic models, each of which was taken through 30 simulations (750 total simulations), provide a basis for defining possible ranges of static and dynamic production characteristics in carbonate shoreface reservoirs. Representative models illustrate changes in facies within (Figure 6A) and among (Figure 6B) clinoforms, as well as changes in porosity (Figure 6C, D), and permeability (Figure 6E, F).

Simulation results reveal considerable variability among the 25 models. Data of the p50 for suites of simulations of each geologic model show that: 1) OOIP varies from less than 23 million barrels of oil (MMBO) to almost 65 MMBO, almost three-fold change; 2) production rate ranges from ~0.8 thousand barrels of oil (MBO)/day to > 10 MBO/day, more than an order of magnitude; and 3) cumulative production differs by more an order of magnitude, from < 400 MBO to > 4.5 MMBO (Figure 7).

Similarly, within each geologic model in which the basic geologic parameters remained consistent, the series of 30 simulations provides a measure of variability among realizations of that framework; this measure might be characterized loosely as production uncertainty. One

metric to assess the variability among realizations of the same model, is the difference between minimum and maximum measured output, expressed as a proportion of the minimum (Figure 8). Describing the data in this manner suggests that OOIP varies markedly, with up to 23.3% difference between minimum and maximum values. Production rate and cumulative oil vary among simulation suites for an individual geologic model as well, by up to 313% and 510%, respectively (high variance permeability model). The data suggest that, aside from permeability variance models, models with highly variable (high standard deviation) porosity distributions (models ending in -H) have more variable production attributes than other models.

IMPACT OF GEOLOGIC PARAMETERS ON PRODUCTION

The results of simulation models reveal a broad range of possible static and dynamic attributes among the suite of geologic models (Figure 9). Since the models were designed to capture a spectrum of geologically plausible scenarios and were varied systematically, they also collectively serve as a means to isolate and evaluate the influence of specific parameters or parameter sets.

Influence of stratigraphic geometry

To evaluate the influence of stratigraphic depositional geometries on production characteristics, consider data from: 1) the base model (Model 113HL, with 1:1:3 foreshore:upper shoreface:lower shoreface proportions in clinoform geometry, high porosity, and low variability [Table 3]); 2) a layer-cake model with the same overall facies proportions, porosity, and porosity variability, but with no clinoforms (Model 113LC); 3) a model with facies proportions, geometries and porosity histograms identical to the base model, but with facies distributed stochastically (Model SG-HL); and 4) a model with facies proportions and porosity histograms

the same as the base model, but with no geometries and purely stochastic facies, and therefore porosity distribution (Model S-HL).

A plot of OOIP versus production rate by model (Figure 9A) reveals broadly similar range in OOIP among realizations of simulation models, and production rates that vary by ~2%; cumulative production shows broadly similar trends (not illustrated). These data also reveal that in general terms, for a similar OOIP, the purely stochastic models include higher production rates than layer-cake models or models with geometries.

Comparing production attributes among geologic models (p50 for all 30 simulations of the four geologic models) reveals the influence of stratigraphic geometry (Figure 9B). For example, relative to the base model, OOIP and production rate is increased in each of the models; cumulative production increases marginally in the stochastic models (< 1.4%) and decreases (< 1%) in the layer-cake model. No correlation is evident between the OOIP and production characteristics.

Interpretation: Many models of shoreface reservoirs, both clastic and carbonate, evaluate a layer-cake stratal layering scheme (e.g., Jackson et al., 2009). A layer-cake interpretation has potentially substantial implications that can lead to modeling results inconsistent with geological reality, and drive variability in predicted production. Instead of the horizontal strata of the layer-cake interpretation, clinoform geometries incorporate inclined layering, which can impact reservoir connectivity (when associated with impermeable barriers, not included in these particular models), drainage efficiency (Kjonsvik et al., 1994; Yose et al., 2006; Jackson et al., 2009), and ultimately, production attributes.

Results of simulations of these carbonate shoreface models suggest, however, that inclusion of clinoforms geometries *alone* does not markedly impact production. Production is

impacted, however, when clinoform-bounding surfaces are accompanied by diagenetic alterations (e.g. exposure surfaces that form conduits or barriers) that compartmentalize the reservoir (see below).

Effect of facies proportions

To explore how vertical (facies proportions) and lateral (plan-view changes in clinoform curvature) facies changes influence production characteristics, several scenarios with constant porosity and permeability distribution for each facies and clinoform geometry included: 1) the base model (same as above, Model 113HL, with 1:1:3 (foreshore:upper shoreface:lower shoreface) proportions in clinoform geometry, high porosity, low variability); 2) a model with 1:3:1 (foreshore:upper shoreface:lower shoreface) proportions (Model 131), but same geometries and facies-porosity relations; 3) a model with 1:2:2 (foreshore:upper shoreface:lower shoreface) proportions (Model 122) and the same geometry and facies-porosity relations. Collectively, these three models might also be considered to represent increasing energy levels, with progressively more foreshore and upper shoreface (from 40% abundance in Model 113HL to 80% abundance in Model 131). A final model 4) has the same facies proportions as the base model, but alters the plan-view curvature of the clinoforms. This model used an additional 16 pseudo-logs to produce the arcuate, rather than purely linear (e.g., strike parallel), clinoforms (cf. Figure 3).

A plot of OOIP versus production rate by model (Figure 9C) reveals the character of production variability among models. For example, increasing proportions of (more porous) high energy deposits (foreshore and upper shoreface) results in greater OOIP and higher production rates, and values which follow a general linear trend on an OOIP versus production rate plot. The two models with constant facies proportions but distinct plan-view geometries

(Model 113-HL and Model 113Arc), however, reveal no change in OOIP, but an increase in production rate in the arcuate ridge sets (Figure 9C; cumulative oil [not shown] follows a comparable trend). Variability among simulations, for the same model, range from 0.6% (production rate and cumulative production) to 2.4% (OOIP).

Production attributes among geologic models (p50 for all 30 simulations of the four geologic models) reveals the influence of facies proportions and plan-view geometry (Figure 9D). The data reveal that p50 OOIP among models varies by almost 31%. The impact on production rate and cumulative production (p50s for all 30 simulations of each model) is less pronounced (less than 7.5% and 5.5%, respectively).

Interpretation: The observation that increased OOIP in this suite of models is closely related to proportion of porous high energy deposits is not surprising. Nonetheless, this increase is not accompanied by a proportionally comparable increase in production rate or cumulative production. The increases in these production metrics are comparable to those present in the arcuate ridge set model, because the arcuate trend permits the production well to penetrate more than one ridge set. Where plan-view geometries are more complex, with compartmentalized ridge sets (cf. Figure 3) (even in the absence of diagenesis), results may have been even more divergent.

Impact of diagenetic surfaces and bodies

To assess the possible impact of diagenesis on production characteristics, data from five models capture a range of plausible geologic scenarios. As the diagenetic modification associated with subaerial exposure can enhance or degrade rock properties such as porosity and permeability (Moore, 1997; Yose et al., 2006), two models provide end-member evaluation of the impact of subaerial exposure surfaces. These models use the same inputs as the base model,

except for the addition of a 0.5 m zone between ridge sets representing an exposure surface. In one (Model HL-ESL), an exposure surface (a continuous layer one cell thick) was assigned lower porosity and permeability values (0.1% and 0 md, respectively) to simulate a transmissibility barrier between ridge sets. In contrast, the exposure surface for the other (Model HL-ESH) was assigned higher porosity and permeability values (30% and 1,000 md, respectively) to simulate the potential for exposure to enhance porosity and permeability, and the altered zone to act as a fluid flow conduit. As an aside, these thin zones bounding clinoforms might also be envisioned as non-diagenetic layers as well, such as flooding surfaces that form less permeable barriers or as coarse lags that form thin flow-enhancing layers.

The other two models simulate simplified, geologically plausible scenarios related to diagenetic alteration of stratigraphic intervals. A first scenario (Model HoH-PL) includes an exposure surface accompanied by a decrease in porosity (mimicking “cementation”) in the underlying, older ridge sets. The second scenario (Model HoL-PH) simulates a situation in which the exposure surface acts as a barrier that protects porosity in the older ridge sets (preserving porosity and permeability), whereas the younger ridge set is subjected to porosity-reducing cementation.

A plot of OOIP versus production rate by model (Figure 9G) reveals that for the two models that explore the impact of exposure surfaces, all realizations have similar OOIP of around 47 MMBO. Production rates are higher for the porosity flow conduit layer (Model HL-ESH, rates nearing 10 MBO/day) and lower for the porosity flow barrier scenario (Model HL-ESL, rate of < 8.5 MBO/day) relative to the base model (rates ~9.25 MBO/day).

This plot also illustrates that the diagenetic interval scenarios have considerable spread in both OOIP and production rate (Figure 9G). Relative to the base model, OOIP and production

rate are decreased in all scenarios, with up to 15 MMBO difference in OOIP and 8 MBO/day decrease in production rate.

Comparing production attributes (p50 for all 30 simulations of each model) of these four geologic models with the base model, reveals the relative impact of diagenesis (Figure 9H). As expected, OOIP varies by 37.8%, associated with variations in porosity among models. In the scenario in which the exposure surface is a transmissibility-enhancing conduit, production rates increase by 6.7% and cumulative production increases by 7.3%. In contrast, in transmissibility-barrier subaerial exposure surface scenario, production rates and cumulative production decrease by 10.5% and 7.7%, respectively. The model with a less porous youngest zone (Model HoL-PH) includes similar decreases in production rate (10.8%) and cumulative production (8.1%) relative to the base model, as OOIP is markedly decreased (16.6%), reflecting the lower-porosity youngest body. In contrast, the scenario with the lower porosity below the subaerial exposure surface (Model HoH-PL) includes markedly decreased static and dynamic production attributes; relative to the base model it has decreases in cumulative production of 22.3%, production rate declines 33.7%, and OOIP is down 35.7%.

Interpretation: Carbonate shoreface successions, such as those on Long Cay, commonly are bounded by subaerial exposure surfaces. In the Bahamas, these types of surfaces separate Pleistocene and Holocene deposits (Aurell et al., 1995; Carew and Mylroie, 1995; Aalto and Dill, 1996; Wanless and Dravis, 2008), and comparable surfaces have been recognized throughout the stratigraphic record, where they can form sequence boundaries.

This modeling assessment considered several subaerial exposure surface and diagenetic body scenarios. Comparing the two subaerial exposure surface models reveals the important role of even thin diagenetically enhanced or degraded porosity and permeability on production rates

and cumulative production (> 17% variability in these models relative to the base model), even though OOIP is essentially the same.

As they define clinoform-bounding surfaces, and separate units with different diagenetic histories, sequence boundaries are a possible driver of simplified diagenetically modified geometric- and facies-related heterogeneity (e.g., Wach et al., 2004), and can compartmentalize reservoirs. Compartmentalization can be associated with enhanced variability within and among reservoir sequences, such as those captured in the diagenetic interval scenarios. This variability (and precisely where the production well lies relative to these sequence boundaries and diagenetically modified facies bodies) leads to production variability of up to 22% in cumulative production and 33% in production rates. In net, simulation results illustrate that although clinoform geometries *alone* do not markedly impact production (as discussed above), clinoforms associated with changes in porosity (due to diagenesis) lead to pronounced variability in production, whether associated with laterally continuous diagenetic surfaces or diagenetically altered intervals.

Comparing among models, it is also interesting to note that although the flow-barrier exposure surface scenario (Model HL-ESL) and the less porous youngest zone scenario (Model HoL-PH) include distinct OOIP (> 15% difference), the production rate and cumulative production metrics are comparable (Figure 9H). This apparent contradiction is related to the overall volumetric decrease in porosity, but this youngest interval is not penetrated by the well (it is in a clinoform offset from the well), and so it exerts limited influence on changes in production.

Impact of porosity variability

Results from several models allow exploration of the impact of porosity and variability in porosity on production characteristics. These models investigate these parameters by varying mean porosity (low and high) and standard deviations of porosity (low and high) (see Table 3), with facies proportions, clinoform geometries, and permeability consistent with the base model. These models (113 prefix) are named with reference to mean porosity (first letter) and porosity standard deviation (second letter); therefore, for example, Model 113HL has high porosity and low standard deviation, Model 113LM has low porosity and medium standard deviation, and so on.

Results of all simulations and scenarios reveal that OOIPs of the low porosity models are centered around 25 MMBO, whereas the high porosity models range up to just over 50 MMBO, consistent with the overall increase in mean porosity (Figure 9E). The production rates do not change as markedly, however, with an increase from just under 8 MBO/day for the low porosity models to just over 9 MBO/day for the high porosity models. A cross plot of OOIP versus production rates (Figure 9E) show a positive correlation between these static and dynamic metrics. Among the 30 simulations for each model, production rate varies by 5.3%, cumulative production differs by 5.3%, and OOIP changes by 23.3%; this variability in OOIP is some of the highest intra-model range of all the different classes of geologic models discussed in this paper.

A plot comparing simulation p50 values with the base model (Figure 9F) reveals that, for the high mean porosity models (Models 113HH; Model 113HL is the base model to which the others are compared, and so is not illustrated), there is < 1% variation in all production metrics. These results show that for models with high mean porosity values, an increase in variance (from standard deviation of 1 to 5) does not markedly impact production. In contrast,

models with low mean porosity values (Models 113LL and 113LH) include a decrease in OOIP (up to 50.3%). Production rates and cumulative production for 'low' porosity models vary more from the base model in absolute terms (deviating by up to 17.3% and 13.8%, respectively), and include more variability among models (production rate by 3.4%; cumulative production by 3%) than the high porosity models (which were all within 1%).

Interpretation: The high porosity models all included high OOIP, and generally similar production rates and cumulative production, suggesting that production was not limited in any way by low-flow streaks. In contrast, the low porosity simulations included lower OOIP, and more divergent production rates and cumulative production. These changes may be related to increased occurrence of laterally discontinuous, low-porosity lenses that partition the reservoir and separate thin units of high porosity. Nonetheless, although OOIP varies considerably, production rates and cumulative production for are not as markedly different from the base model compared to models that capture other controls.

Impact of permeability

To unravel the possible influence of permeability, three models provide data: one model for the range of values and two models to assess variability. Since the base model provides the framework, facies proportions and clinoform geometries are consistent with the base model. The first model (Model Oomoldic) simulates an oomoldic reservoir. Although oomoldic reservoirs can include a range of permeability, most exhibit permeability lower than interparticle porosity-dominated reservoirs with comparable porosity (e.g., Watney, 1980; Lucia, 2007). All other input held constant, the oomoldic model includes an order of magnitude decrease in permeability (I and J of 20 md and K of 2 md). The two permeability variance models (Models 113kLL, 113kLH) use similar mean permeability values as the base model but vary the permeability

standard deviation (low and high) (Table 3). The base model p50 realization provides the framework for porosity values and distribution for the variance models.

Observation of the plot of OOIP versus production rate by model (Figure 9I) reveals that, although there is little variance in OOIP, there is a marked increase in the scatter in production rate among the three permeability models. This trend is most evident in the models which evaluate the variability of permeability, and have rates ranging from 2.6 to 10.8 MBO/day (Model 113kLH). As porosity was held constant for these models, this variability is not reflected directly in OOIP. Data also reveal the substantial reduction in production rates between the base (interparticle) and oomoldic models, from ~ 9.2 MBO/day from the base model to rates ~1.4 MBO/day for the oomoldic scenario.

Comparing production attributes among permeability models (p50 for all 30 simulations of the four geologic models) reveals the influence of permeability values and variance (Figure 9J). The oomoldic scenario has an OOIP similar to the base model, but shows a pronounced change in production characteristics, with production rates decreased by 85% and cumulative production down by 86%. Introducing permeability variability (Models 113kLL and 113kLH), production rates and cumulative production decrease by as much as 29% and 33%, respectively. For these models, OOIP was constant; therefore variation in cumulative production and production rates is independent of OOIP.

Interpretation: Analog oolitic reservoirs exhibit a spectrum of permeability ranges (both mean values and variance) (Cussey and Friedman, 1977; Benson and Mancini, 1982; Druckman and Moore, 1985; Watney and French, 1988; Alsharhan, 1993; Mougenot, 1999; Davies et al., 2000; Sahin and Saner, 2001; Lindsay et al., 2006; Figure 4). The oomoldic scenario with the lower permeability is consistent with trends in high porosity, low permeability reservoirs in

which high porosity (and OOIP) is not reflected in production (e.g., Watney 1980). The other two models, which vary permeability to different levels, also result in decreased production. Similarly, the variation among models illustrates the likely importance of streaks, pods, or lenses of low permeability (e.g., cells with lower than average permeability, perhaps thin more muddy layers, different or uneven cementation or dissolution) that create a more tortuous or at least more heterogeneous flow path, hence decreasing rates.

Summary of geologic controls

The suite of geologic models reveals the distinct roles of various geological scenarios on the absolute values and variability of static and dynamic production metrics. A plot of change in these metrics as a function of change from the base model for these simulations (Figure 10) reveals several interesting factors. First, in terms of OOIP, the models with higher average porosity or facies proportions with greater abundance of high-energy porous deposits (e.g., Models 131, 122) result in OOIP greater than those with lower porosity or a greater proportion of lower-energy deposits (e.g., Models 113LL, 113LH) (Figure 10). Second, in the context of production rates or cumulative production, the most important influence is permeability (Models 113kLL, 113kLH, and Oomoldic). Aside from those changes (e.g., for constant permeability), the models that altered how porosity was distributed (with changes in facies proportions, or the distinct porosity zones) or segmented (by the baffles or conduits provided by subaerial exposure surfaces) impacted change in production metrics the most. Finally, for constant permeability (eliminating the oomoldic and permeability models) the changes in p50 OOIP are correlated with p50 cumulative production ($R^2 = 0.77$) and p50 production rate ($R^2 = 0.74$).

CONCLUSIONS

Such geological controls as stratigraphy, facies, and diagenesis influence production trends of carbonate reservoirs. Designed to capture a spectrum of potential geological variability of carbonate shorefaces, a suite of simple geologic models carried through to reservoir simulation permitted systematic and quantitative assessment of the influence of these geological factors on initial production.

The data derived from these simulations illustrate how the influence of geologic factors range in nature and scope on both static and dynamic production metrics. For example, models with *stochastic facies distribution* (either with horizontal parallel [layer cake] zones or with clinoform bounding surfaces; mean porosity, facies proportions, etc. similar to a base model) have production rates and cumulative production that differs from the base clinoform model by < 2%. Analogously, *depositional geometries* (i.e., clinoforms versus layer cake) *alone* do not have a marked impact on OOIP or production rates. If associated with a continuous, impermeable barrier (e.g., cemented *subaerial exposure surface* or a flooding surface) that compartmentalizes the reservoir, however, these bounding surfaces impact production. Although OOIP is not impacted markedly (< 1% change), production rates and cumulative production can decrease in excess of 7% as a function of the impact of one thin zone alone. This influence can be emphasized if the impermeable barrier is linked to enhanced *diagenesis* (e.g., cementation that decreases porosity) to create a distinct stratigraphically constrained *diagenetic body* (e.g., clinoform with distinct porosity) in underlying deposits. Simulations suggest that this impact alone can result in decreases in OOIP (up to 36%), and corresponding declines in production rate (up to 33%), and cumulative production (up to 23%). Since facies include distinct petrophysical characteristics in the models, changing *facies proportions* impact OOIP, production rate, and

cumulative production; greater proportions of high-energy porous and permeable upper shoreface and foreshore strata result in increased OOIP and production. Changes in *porosity* obviously directly impact OOIP, although mean porosity impacts production rate and cumulative production more than porosity variance (e.g., changing the porosity standard deviation). *Permeability* is the most important control on production rate; however, it is also the parameter in which different realizations of the same geologic model have the greatest range (e.g., it includes the greatest risk). The strong positive correlation between p50 of OOIP and p50 of production metrics (among simulations of a given geologic model) suggest that production rates are sensitive to heterogeneities that influence OOIP (i.e., stacking patterns, porosity distribution), with the outliers representing the impact of diagenetic surfaces and moldic porosity (high porosity, low permeability).

Ranking of relative importance of the geologic parameters varies by evaluation metric. The influence of geological parameters on *OOIP*, a static metric, ranges from least important to most important: permeability distribution, depositional geometry, diagenesis (but only if associated with diagenetic bodies), stacking patterns, to porosity distribution. For dynamic metrics (*production rate* and *cumulative production*), geological parameters exert an influence that ranges from (in order, least to most important) depositional geometry, diagenetic intervals and diagenetic surfaces, stacking patterns, porosity distribution, to permeability distribution.

Quantifying and ranking how geologic heterogeneities impact production in carbonate shoreface reservoirs provides another means for geologists to focus observations on the geological factors that actually make a difference. As such, quantifying the influence of geologic

heterogeneity on production also ultimately aids hydrocarbon development and production strategies through providing more effective and accurate reservoir trend predictions.

REFERENCES

Aalto, K.R., and Dill, R.F., 1996, Late Pleistocene stratigraphy of a carbonate platform margin, Exumas, Bahamas: Sedimentary Geology, v. 103, p. 129-143.

Agada, S., Chen, F., Geiger, S., Toigulova, G., Agar, S., Shekhar, R., Benson, G., Hehmeyer, O., Amour, F., Mutti, M., Christ, N., and Immenhauser, A., 2014, Numerical simulation of fluid flow processes in a 3D high-resolution carbonate reservoir analogue: Petroleum Geoscience, v. 20, p. 125–142.

Agar, S.M., and Hampson, G.J., 2014, Fundamental controls on flow in carbonates: an introduction: Petroleum Geoscience, v. 20, p, 3–5.

Agar, S.M., Geiger-Boschung, S., Matthai, S.K., Always, R., Tomas, S., Immenhauser, A., Shekhar, R., Paul, J., Benson, G., Karcz, Z., and Kabiri, L., 2009, The impact of hierarchical fracture networks on flow partitioning in carbonate reservoirs: Examples based on a Jurassic carbonate analog from the High Atlas: OnePetro SPE #135135, 19 p.

Alsharhan, A., 1993, Asab Field--United Arab Emirates, Rub Al Khali Basin, Abu Dhabi, *in* Foster, N.H., and Beaumont, E.A., eds., Structural Traps VIII: AAPG Treatise of Petroleum Geology, Atlas of Oil and Gas Fields, p. 69–97.

Amour, F., Mutti, M., Christ, N., Immenhauser, A., Benson, G.S., Agar, S.M., Tomas, S., and Kabiri, L., 2012, Capturing and modeling metre-scale spatial facies heterogeneity in a Jurassic ramp setting (Central High Atlas, Morocco): Sedimentology, v. 59, p. 1158–1189.

Amour, F., Mutti, M., Christ, N. Immenhauser, A., Agar, S.M, Benson, G.S., Tomas, S., Alway, R., and Kabiri, L.,2013, Outcrop analog for an oolitic carbonate ramp reservoir: A scale-dependent geologic modelling approach based on stratigraphic hierarchy: AAPG Bulletin, v. 97, p. 845–871.

Arakel, A.V., 1982, Genesis of calcrete in Quaternary soil profiles, Hutt and Leeman Lagoons, Western Australia: Journal of Sedimentary Petrology, v. 52, p. 109-125.

Aurell, M., McNeill, D.F., Guyomard, T., and Kindler, P., 1995, Pleistocene shallowing-upward sequences in New Providence, Bahamas: Signature of high-frequency sea-level fluctuations in shallow carbonate platforms: Journal of Sedimentary Research, v. 65, p. 170–182.

Benson, D.J., and Mancini, E.A., 1982, Petrology and reservoir characteristics of the Smackover Formation, Hatter's Pond Field: implications for Smackover exploration in southwestern Alabama: Gulf Coast Association of Geological Societies Transactions, v. 32, p. 67–75.

Cao, R., Ma, Y.Z., Gomez, E., 2014. Geostatistical applications in petroleum reservoir modeling: Southern African Institute of Mining and Metallurgy, v. 114, p. 625–629.

Carew, J. L. and J. E. Mylroie, 1995, Depositional model and stratigraphy for the Quaternary geology of the Bahama Islands, *in* Curran, H.A., and White, B., eds., Terrestrial and

Shallow Marine Geology of the Bahamas and Bermuda: Geological Society of America, Special Paper No. 300, p. 5-32.

Carrasco, B.N., Portella, R.C.M., and Becker, M.R., 2001, Studies of sedimentological heterogeneities and their impact in fluid flow simulation: Society of Petroleum Engineers, paper number 69472, p. 1-13.

Cussey, R., and Friedman, G.M., 1977, Patterns of porosity and cement in ooid reservoirs in Dogger (Middle Jurassic) of France: AAPG Bulletin, v. 61, p. 511–518.

Davies, R., Hollis, C., Bishop, C., Gaur, R., and Haider, A.A., 2000, Reservoir geology of the middle Minagish Member (Minagish Oolite), Umm Gudair field, Kuwait, in Alsharhan, A.S., and Scott, R.W., eds., Middle East Models of Jurassic/Cretaceous Carbonate Systems: SEPM Special Publication, v. 69, p. 273–286.

Deng, H., Aguilera, R., and Settari, A., 2011, An integrated workflow for reservoir modeling and flow simulation of Nikanassin tight gas reservoir in the Western Canada sedimentary Basin: SPE paper 146953, p. 1-26

Deutsch, C.V., 2002, Geostatistical reservoir modeling: New York, Oxford University Press, 376 p.

Dickson, J.A.D., and Saller, A., 1995, Identification of subaerial exposure surfaces and porosity preservation in Pennsylvanian and Lower Permian shelf limestones, eastern Central Basin Platform, Texas, *in* Budd, D.A., Saller, A.H., and Harris, P.M., eds., Unconformities and Porosity in Carbonate Strata, AAPG Memoir 63, p. 239-258.

Druckman, Y., and Moore Jr., C.H., 1985, Late subsurface secondary porosity in a Jurassic grainstone reservoir, Smackover Formation, Mt. Vernon field, southern Arkansas, *in* Roehl, P.O., and Choquette, P.W., eds., Carbonate Petroleum Reservoirs: Springer, p. 369–383.

Eltom, H., Makkawi, M., Abdullatif, O., and Alramadan, K., 2012, High-resolution facies and porosity models of the upper Jurassic Arab-D carbonate reservoir using outcrop analogue, central Saudi Arabia: Arabian Journal of Geosciences, v. 6, p. 4323–4335.

Esteban, M., and Klappa, C.F., 1983, Subaerial exposure environment, *in* Scholle, P.A., Bebout, D.G., and Moore, C.H., eds., Carbonate Depositional Environments: AAPG Memoir 33, p. 1–54.

Falivene, O., Arbués, P., Howell, J., Muñoz, J.A., Fernández, O., and Marzo, N., 2006, Hierarchical geocellular facies modeling of a turbidite reservoir analog from the Eocene of the Ainsa Basin, NE Spain: Marine and Petroleum Geology, v. 23, p. 679–701.

Fitch, P.J.R., Jackson, M.D., Hampson, G.J. and John, C.M. 2014, Interaction of stratigraphic and sedimentological heterogeneities with flow in carbonate ramp reservoirs: Impact of fluid properties and production strategy: Petroleum Geoscience, v. 20, p. 7–26.

Goldhammer, R.K., and Elmore, R.D., 1984, Paleosols capping regressive carbonate cycles in the Pennsylvanian Black Prince Limestone, Arizona: Journal of Sedimentary Research: v. 54, p. 1124-1137.

Goldstein, R.H., 1988, Paleosols of Late Pennsylvanian cyclic strata, New Mexico: Sedimentology, v. 35, p. 777-804.

Handford, C.R., and Baria, L., 2007, Geometry and seismic geomorphology of carbonate shoreface clinoforms, Jurassic Smackover Formation, north Louisiana, *in* Davies, R.J., Posamentier, H.W, Wood, L.J, and Cartwright, J.A, eds., Seismic Geomorphology: Applications to Hydrocarbon Exploration and Production: Geological Society of London, Special Publication, v. 277, p. 171-185.

Hearty, P. and Kindler, P., 1993, New perspectives on Bahamian geology: San Salvador Island, Bahamas: Journal of Coastal Research, v. 9, p. 577-594.

Hearty, P.J. and Kindler, P., 1997, The stratigraphy and surficial geology of New Providence and surrounding islands, Bahamas: Journal of Coastal Research, v. 13, p. 798-812.

Inden, R.F., and Moore, C.H., 1983, Beach environment, *in* Scholle, P.A., Bebout, D.G., and Moore, C.H., eds., Carbonate Depositional Environments: AAPG Memoir, v. 33, p. 211-265.

Jackson, M.D., Hampson, G.J., and Sech, R.P., 2009, Three-dimensional modeling of a shoreface-shelf parasequences reservoir analog: Part 2. Geologic controls on fluid flow and hydrocarbon recovery: AAPG Bulletin, v. 93, p. 1183-1208.

Jung, A., and Aigner, T., 2012, Carbonate geobodies: Hierarchical classification and database – a new workflow for 3D reservoir modelling: Journal of Petroleum Geology, v. 35, p. 49–66.

Kerans, C. and Tinker, S.W., 1997, Sequence Stratigraphy and Characterization of Carbonate Reservoirs: SEPM Short Course Notes #40, 130 p.

King, M.J., and Mansfield, M., 1999, Flow simulation of geologic models. SPE Reservoir Evaluation and Engineering, v. 2, p. 351-367.

Kjonsvik, D., Doyle, J.D., Jacobsen, T., and Jones, A.D.W., 1994, The effects of sedimentary heterogeneities on production from a shallow marine reservoir - What really matters?: Presented at the 1994 European Petroleum Conference, London, Society of Petroleum Engineers Paper 28445, p. 27–40.

Lindsay, R.F., Cantrell, D.L., Hughes, G.W., Keith, T.H., Mueller III, H.W., and Russell, S.D., 2006, Ghawar Arab-D reservoir: widespread porosity in shoaling-upward carbonate cycles, Saudi Arabia, *in* Harris, P.M., and Weber L.J., eds., Giant hydrocarbon reservoirs of the world: From rocks to reservoir characterization and modeling: AAPG Memoir 88/SEPM Special Publication, p. 97–137.

Lipinski, C.J., Franseen, E.K., and Goldstein, R.H., 2013, Reservoir analog model for oolite-microbialite sequences, Miocene terminal carbonate complex, Spain: AAPG Bulletin, v. 97, p. 2035– 2057.

Lloyd, R.M., Perkins, R.D., and Kerr, S.D., 1987, Beach and shoreface ooid deposition on shallow interior banks, Turks and Caicos Island, British West Indies: Journal of Sedimentary Petrology, v. 57, p. 976–982.

Lucia, J.F., 2007, Carbonate Reservoir Characterization: An Integrated Approach (2nd Edition): Springer, 336 p.

Lui, N., Betancourt, S., and Oliver, D.S., 2001, Assessment of uncertainty assessment methods: SPE paper 71624, p. 1-15.

MacDonald, A.C. and Aasen, J.O. 1994, A prototype procedure for stochastic modelling of facies tract distribution in shoreface reservoirs, *in*, Yarus, J.M. and Chambers, R.L., eds., Stochastic Modelling and Geostatistics, AAPG Bulletin, v. 82, p. 1156–1172.

Moore, C. H., 1997, Sequence stratigraphic framework of Upper Jurassic Oxfordian Smackover Equivalents illustrated by the Humble McKean# 12 core, Buckner Field, southern Arkansas, central Gulf of Mexico, USA, *in* Core Conference: CSPG-SEPM Joint Convention, with the Participation of the Global Sedimentary Geology Program and the Geol. Survey of Canada, p. 305-316

Mougenot, D., 1999, Seismic imaging of a carbonate reservoir; The Dogger of the Villeperdue oil field, Paris Basin, France: Petroleum Geoscience, v. 5, p. 75–82.

Palermo, D., Aigner, T., Nardon, N., and Blendinger, W., 2010, Three-dimensional facies modeling of carbonate sand bodies: Outcrop analog study in an epicontinental basin (Triassic, southwest Germany): AAPG Bulletin, v. 94, p. 475–512

Rankey, E.C., 2014, Contrasts between wave- and tide-dominated oolitic systems: Holocene of Crooked-Acklins Platform, southern Bahamas: Facies, v. 60, p. 405–428.

Sahin, A., and Saner, S., 2001, Statistical distributions and correlations of petrophysical parameters in the Arab-D reservoir, Abqaiq oilfield, Eastern Saudi Arabia: Journal of Petroleum Geology, v. 24, p. 101–114.

Sahin, A., Ghori, S., Ali, A., El-Sahn, H., Hassan, H., Al-Sanounah, A., 1998, Geological controls of variograms in a complex carbonate reservoir, Eastern Province, Saudi Arabia. Mathematical Geology, v. 30, p. 309–322.

Shekhar, R., Sahni, I., Benson, G., Agar, S., Amour, F., Tomas, S., Christ, N., Always, R., Mutti, M., Immenhauser, A., Karcz, Z., and Kabiri, L., 2014, Modelling and simulation of a Jurassic carbonate ramp outcrop, Amellago, High Atlas Mountains, Morocco: Petroleum Geoscience, v. 20, p. 109–124.

Strasser, A., and Davaud, E., 1986, Formation of Holocene limestone sequences by progradation, cementation, and erosion: two examples from the Bahamas: Journal of Sedimentary Research, v. 56, p. 422–428.

Sykes, M.A., Hood, K.C., and Setterdahl, S.I., 2012, Assessment measures: Describing uncertainty accurately, clearly and unambiguously: Search and Discovery article #41023.

Tomás, T., Zitzmann, M., Homann, M., Rumpf, M., Amour, F., Benisek, M., Marcano, G., Mutti, M., and Betzler, C., 2010, From ramp to platform: Building a 3-D model of depositional geometries and facies architectures in transitional carbonates in the Miocene, northern Sardinia: Facies, v. 56, p. 195–210.

Wanless, H.R., and Dravis, J.J., 2008, Pleistocene reefal and oolitic core sequences from West Caicos, Caicos Platform, *in* Morgan, W. and Harris, P.M., eds., Developing Models and Analogs for Isolated Carbonate Platforms—Holocene and Pleistocene Carbonates of Caicos Platform, British West Indies: SEPM Core Workshop, No. 22, p. 171-175.

Watney, W.L., 1980, Cyclic sedimentation of the Lansing-Kansas City groups in northwestern Kansas and southwestern Nebraska: A guide for petroleum exploration: Kansas Geological Survey Bulletin 22, 72 p.

Watney, W.L., and French, J., 1988, Characterization of Carbonate Reservoirs in the Lansing-Kansas City Groups (Upper Pennsylvanian) in Victory Field, Haskell County, Kansas, *in* Goolsby, S. M., and Longman, M. W., eds., Occurrence and Petrophysical Properties of Carbonate Reservoirs in the Rocky Mountain Region: The Rocky Mountain Association of Geologists, p. 27–45.

Yose, L.A., Ruf, A.S., Strohmenger, C.J., Schuelke, J.S., Gombos, A., Al-Hosani, I., Al-Maskary, S., Bloch, G., Al-Mehairi, Y., and Johnson, I.G., 2006, Three-dimensional characterization of a heterogeneous carbonate reservoir, Lower Cretaceous, Abu Dhabi (United Arab Emirates), *in* Harris, P. M. and Weber, L. J., eds., Giant Hydrocarbon Reservoirs of the World: From Rocks to Reservoir Characterization and Modeling: AAPG Memoir 88/SEPM Special Publication, p. 173– 212.

Yose, L.A., Brown, S., Davis, T.L., Eiben, T., Kompanik, G.S., and Maxwell, S.R., 2001, 3- D geologic model of a fractured carbonate reservoir, Norman Wells Field, NWT, Canada: Bulletin of Canadian Petroleum Geology, v. 49, p. 86.

FIGURES

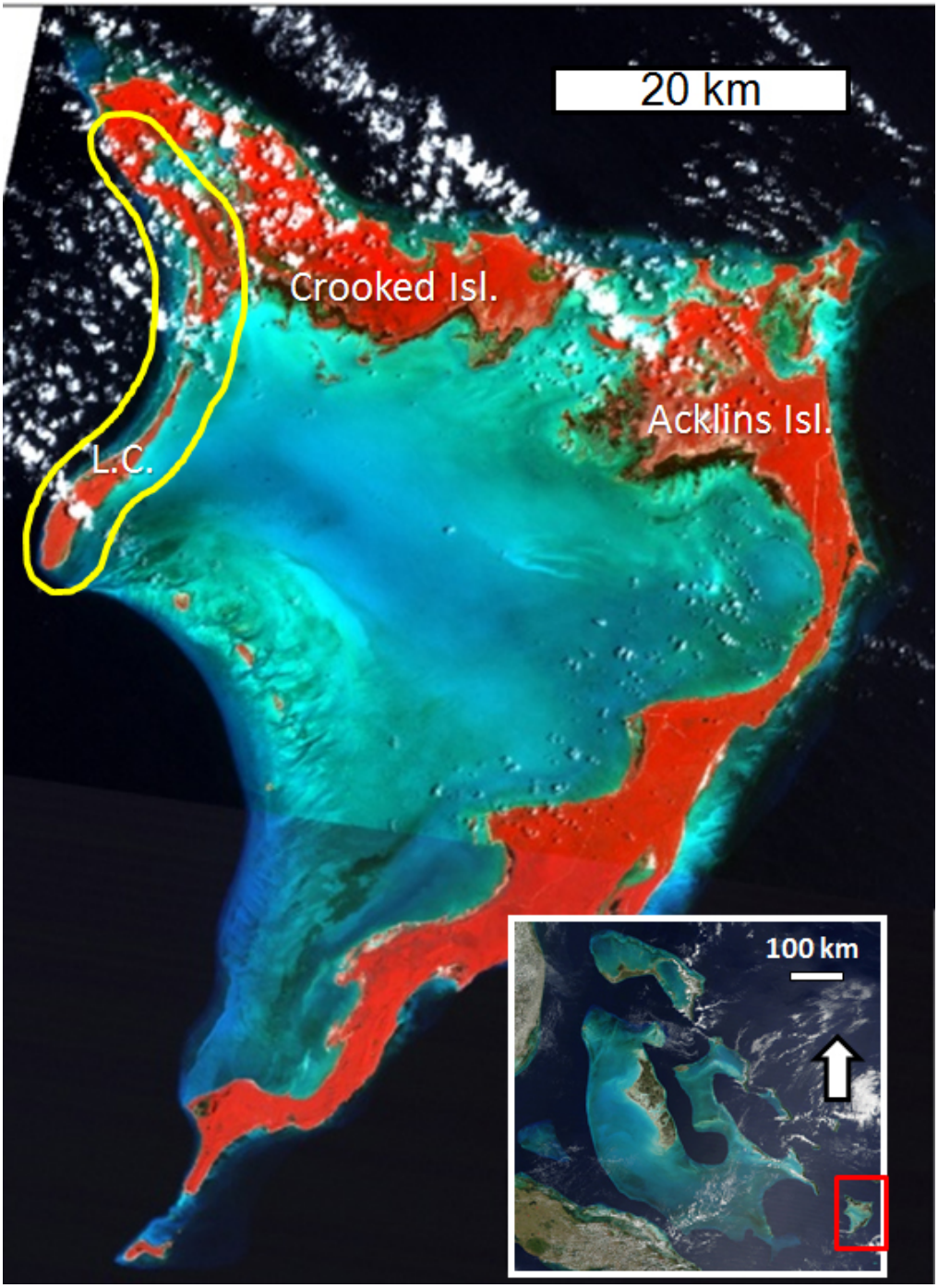

Figure 1. Regional Landsat data illustrating location of the outcrop analog study area on Crooked-Acklins Platform, southern Bahamas. Inset illustrates location of CAP, and yellow box emphasizes the primary field area. L.C. = Long Cay.

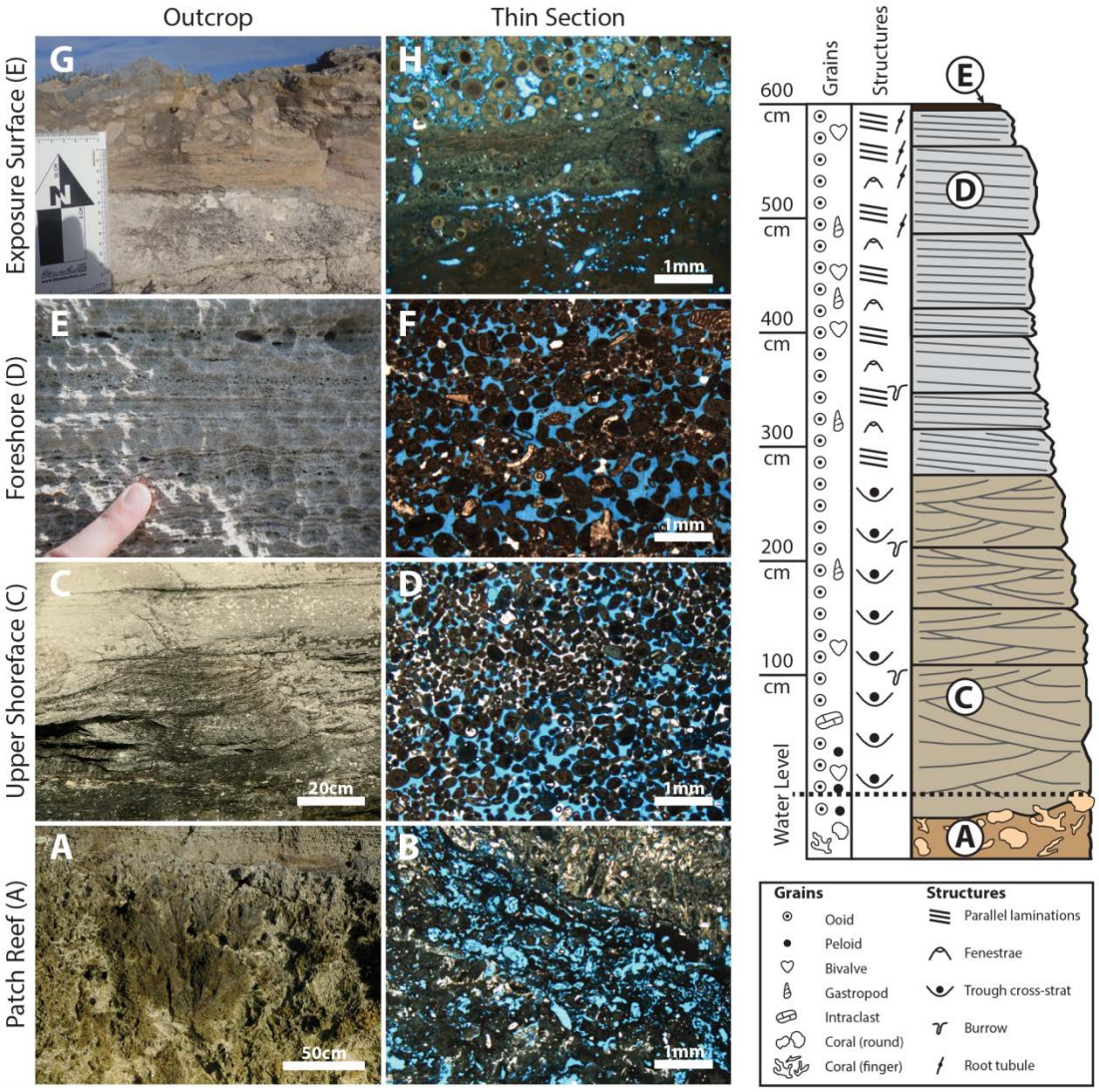

Figure 2. Facies character and representative measured section from southernmost Long Cay. Facies A: A) Outcrop photo showing *in situ* coral growth, B) thin section photomicrograph of skeletal rudstone. (Facies B is not present at the location of this section.) Facies C: C) Outcrop photograph of trough cross-stratified grainstone, D) thin section photomicrograph of moderately well sorted medium sand oolitic grainstone. Facies D: E) Field photo of parallel laminated, fenestral grainstone; F) thin section photomicrograph of coarse-fine layering in laminated grainstone. Facies E: G) Field photo of laminated crust; H) thin section photomicrograph of laminated crust with small root tubules. I) Measured section that includes a Facies A (reef; other areas have Facies B at base, and no reef), overlain by Facies C (an oolitic-skeletal grainstone with troughs; interpreted as upper shoreface), Facies D (an oolitic-skeletal grainstone with fenestrae and low-angle, seaward-dipping laminae; interpreted as foreshore), and Facies E (a subaerial exposure surface). On the basis of the spatial patterns (see Figure 3) of this and comparable measured sections, this Long Cay succession is interpreted to represent a series of prograding carbonate shorefaces.

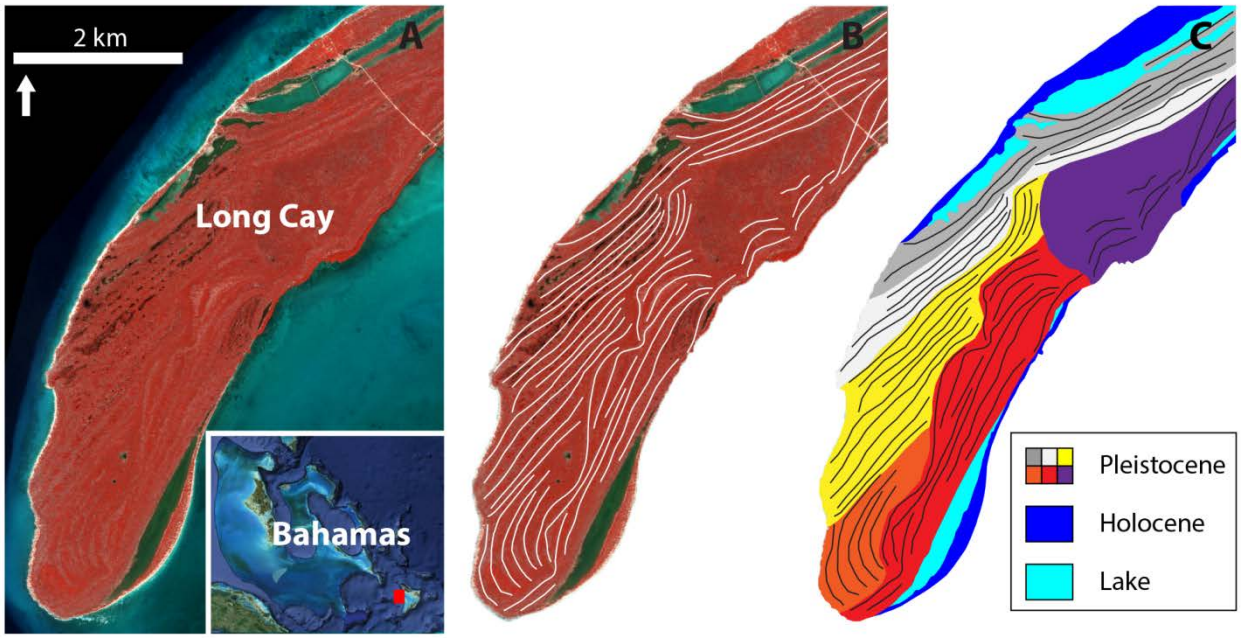

Figure 3. Location and character of outcrop-analog study area, Long Cay, Southern Bahamas. A) Uninterpreted remote sensing image (copyright DigitalGlobe.com) of the southern tip of Long Cay. This island, on the western side of Crooked-Acklins Platform, includes a series of topographic ridges manifest as subtle changes in tone or texture on this image. B) Field-calibrated interpretation of ridge crests. C) Map of ridge sets interpreted from superposition and cross-cutting relationships, illustrating west- and southward accretion. These sets (six, plus Holocene) indicate that although ridges are generally parallel along strike, ridge sets can include complex lateral patterns.

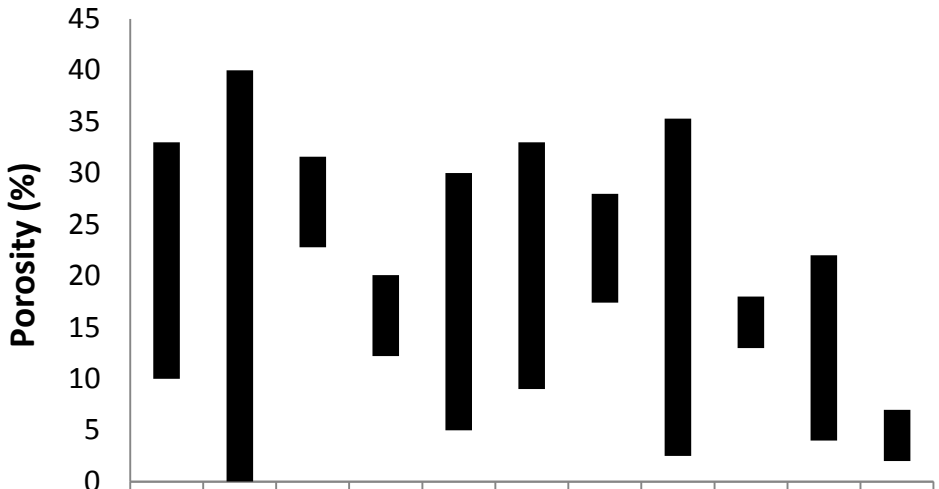

	AD	AD	AF	AF	D	LKC	MO	MO	S	S	S
Max	33	40	31.6	20.1	30	33	28	35.3	18	22	7
Min	10	0.01	22.8	12.2	5	9	17.4	2.5	13	4	2

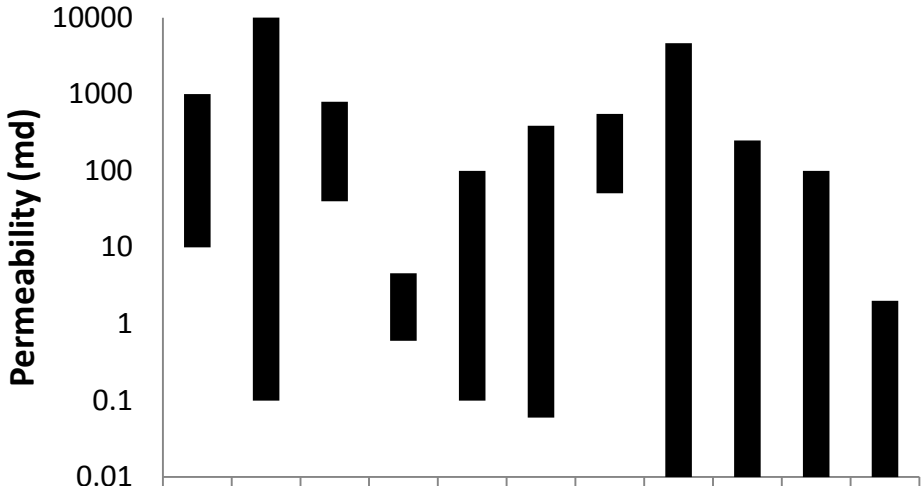

	AD	AD	AF	AF	D	LKC	MO	MO	S	S	S
Max	1000	1000	797	4.6	100	386	553	4652	250	100	2
Min	10	0.1	39.8	0.6	0.1	0.06	51	0.01	0.01	0.01	0.01

Figure 4. Spectrum of ranges of porosity and permeability from subsurface oolitic grainstone reservoirs, illustrating a range of geologically plausible porosity and permeability scenarios. AD = Jurassic Arab-D (Sahin and Saner, 2001; Lindsay et al., 2006); AF = Cretaceous Asab Field (Alsharhan, 1993); D = Jurassic Dogger (Cussey and Friedman, 1977; Mougenot, 1999); LKC = Pennsylvanian Lansing-Kansas City (Watney and French, 1988); MO = Cretaceous Minagish Oolite (Davies et al., 2000); S = Jurassic Smackover (Benson and Mancini, 1982; Druckman and Moore, 1985). Some reservoirs (e.g., AD, AF, MO, S) contain multiple values to further illustrate the variability possible within a reservoir.

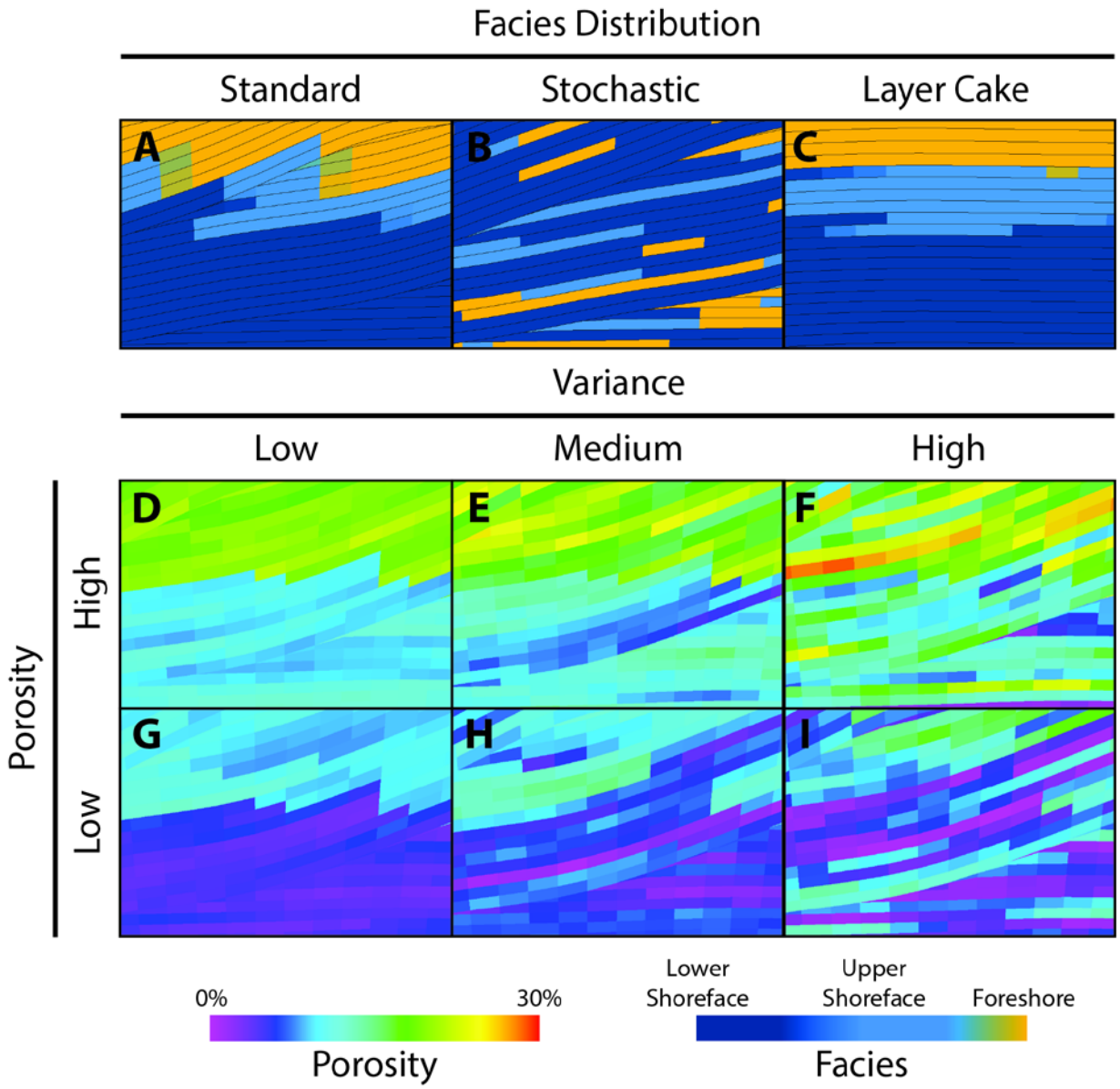

Figure 5. Schematic illustrating variable geological parameters. (A-C) Facies are distributed as (A) shallowing-upward trends within clinoforms; (B) stochastically within clinoforms; or (C) layer-cake (horizontal, parallel) geometry. All use 1:1:3 facies proportions. (D-I) Porosity changes among realizations. Given a constant facies and geometry (here, shallowing-upward clinoforms), models include simulations that change absolute values of porosity (mean porosity) and variability (same mean, different standard deviations) to assess their possible impacts.

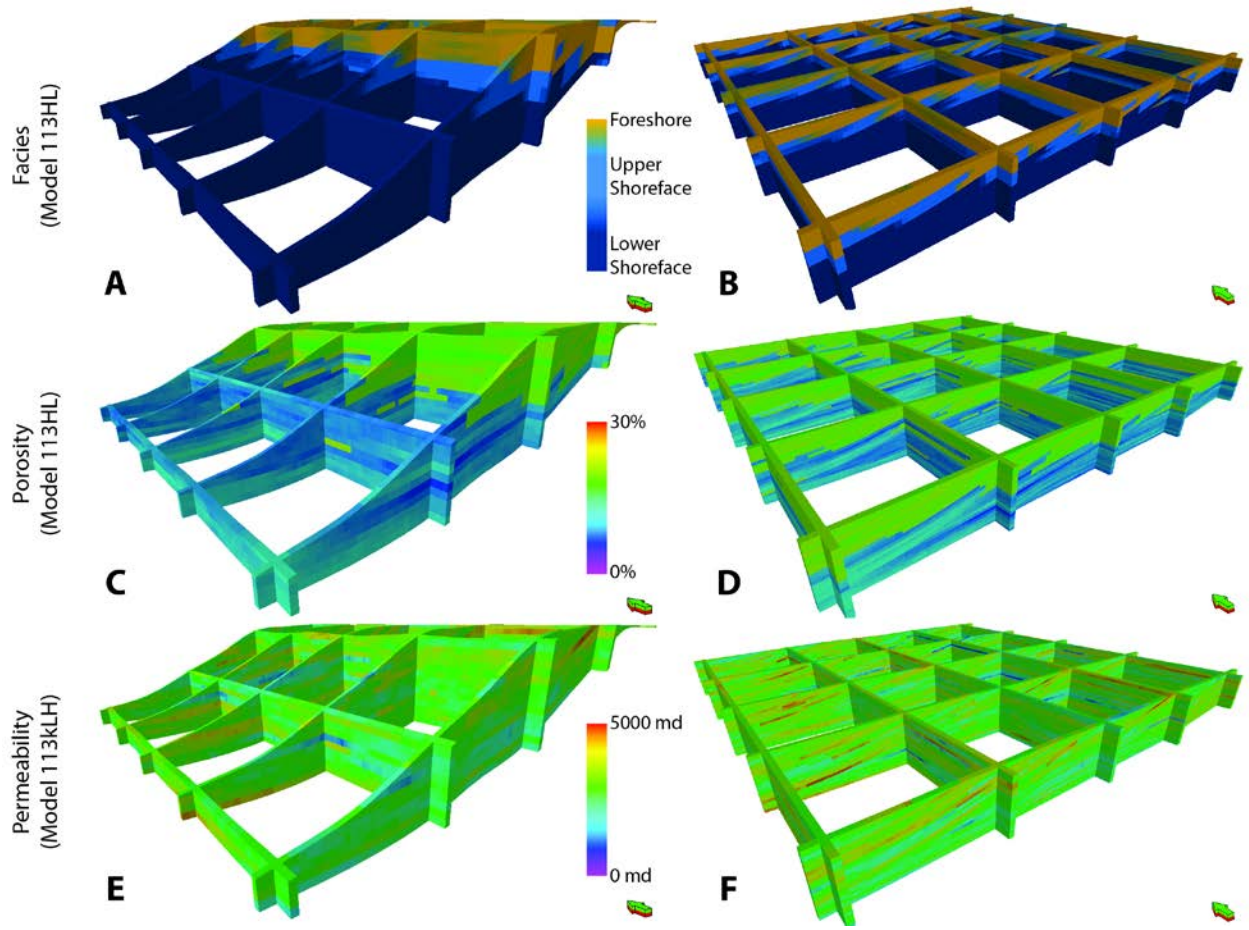

Figure 6. Schematic of the framework of geological models (20 m x 20 m x 1 m grid). A-B) Facies and geometry. Facies for most models are arranged as a series of laterally accreting clinoforms, each of which contains lower shoreface, upper shoreface, and foreshore deposits. C-D) Porosity. Porosity is distributed as a function of facies. E-F) Permeability. Permeability uses a facies-based distribution. For all models, 'fences' are one cell thick (20 m) with a distance between 'fences' of 460 m. Clinoform models (A,C,E) have a vertical exaggeration of 25; full models (B,D,F) have a vertical exaggeration of 10.

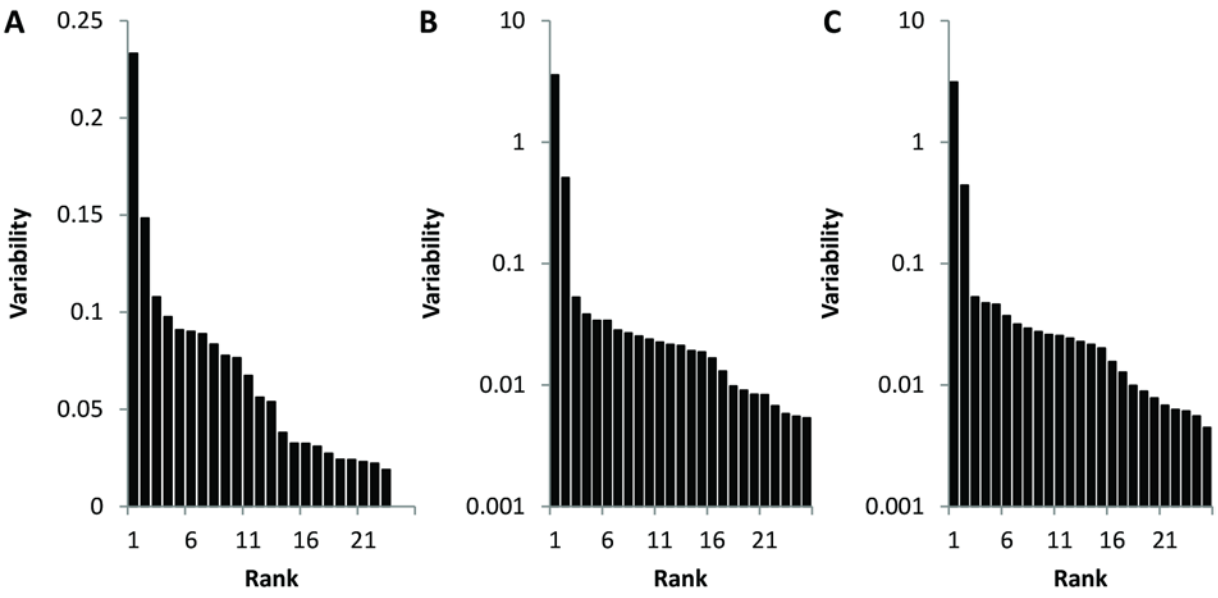

Figure 7. Graphs showing ranked variability data among all models: A) OOIP, B) cumulative production, and c) production rates. Note that the variability for B) and C) use a log scale; this is to accommodate for variability related to permeability models.

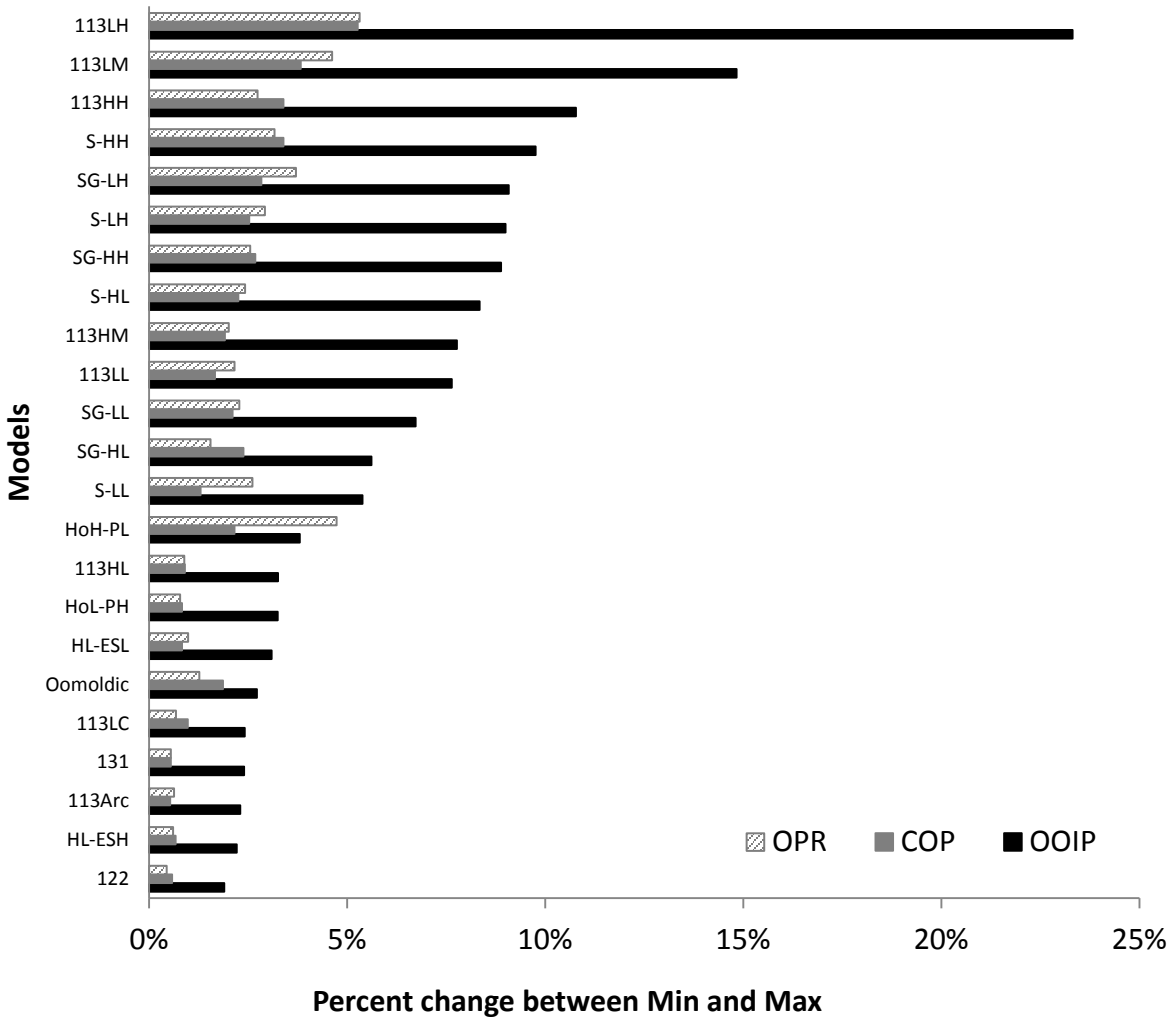

Figure 8. Plot of variability among simulations of a given geologic model, expressed as the difference between maximum and minimum value (OOIP, production rate, cumulative production), normalized to the minimum value. OPR = Oil production rate; COP = Cumulative oil production; OOIP = Original oil in place. This variability metric, which might be considered a measure of risk, shows that even among realizations, many models include OOIP variability of greater than 5%, and production rates and cumulative production greater than 2%.

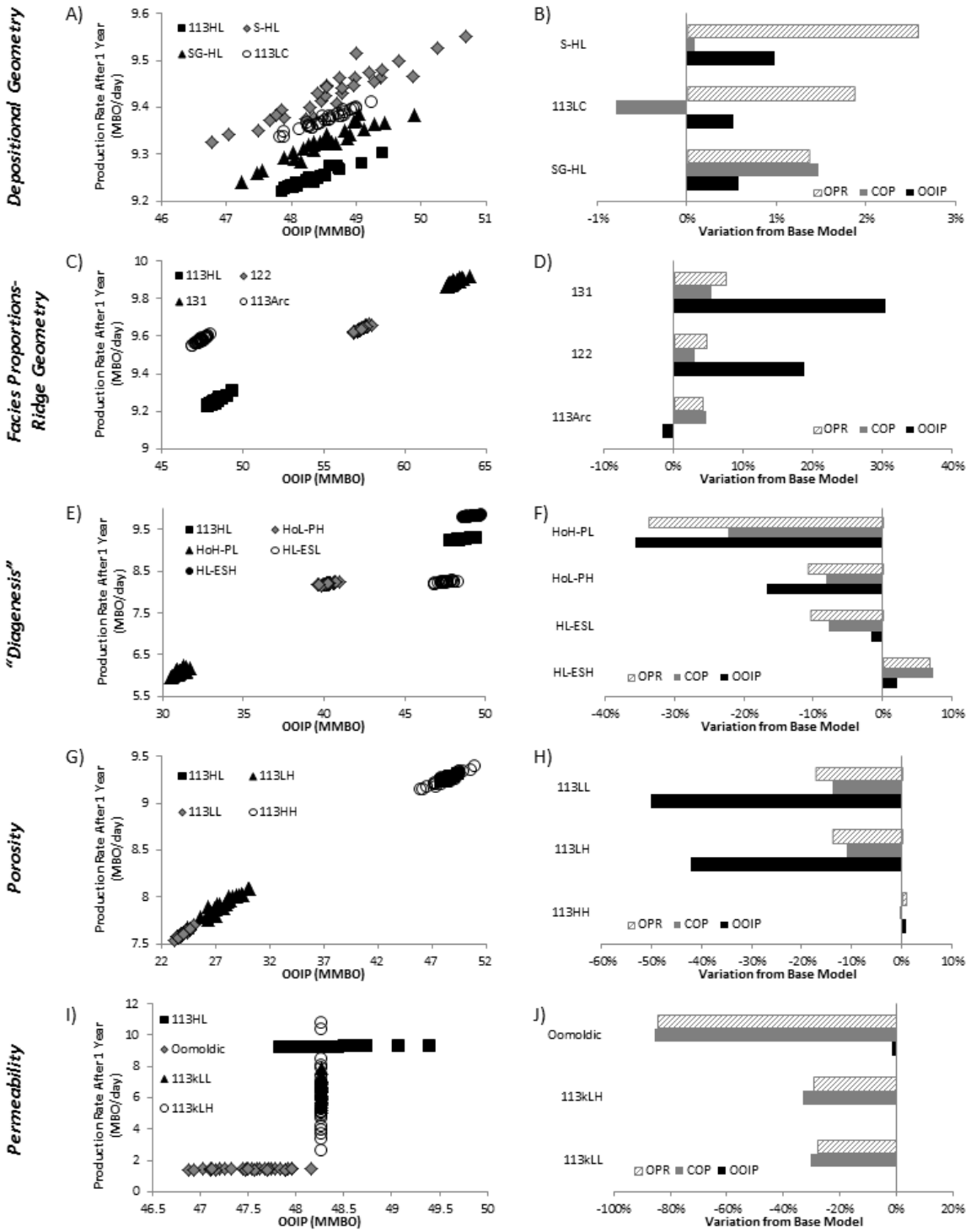

Figure 9. Results from simulation models, organized by geological control. In each suite, variables except for one are constant; thus, comparison among models reveals the absolute (left

column) and relative (expressed as a percentage, normalized to a “base model” (113HL) in each plot) importance of the different parameters. Note that ranges of absolute values (left column) and variation (right column) are different in each row. Model nomenclature is described in the text. OPR = Oil production rate, COP = Cumulative oil production; OOIP = Original oil in place. A-B) Models with distinct depositional geometry; C-D) Models with different facies proportions (Models 122 and 131) and ridge geometry (Model 113Arc); E-F) Models with unique “diagenesis,” manifest as a more (Model HL-ESH) or less (Model HL-ESL) porous-permeable clinoform-bounding layer, older zone with reduced porosity (Model HoH-PL), or younger zone with reduced porosity (Model HoL-PH); G-H) Models with variations in means and standard deviations in porosity; I-J) Models with distinct permeability. Note that the absolute values of OOIP and production rate, as well as the influence on these parameters relative to the base model, change markedly in response to the geological variability. See text for discussion.

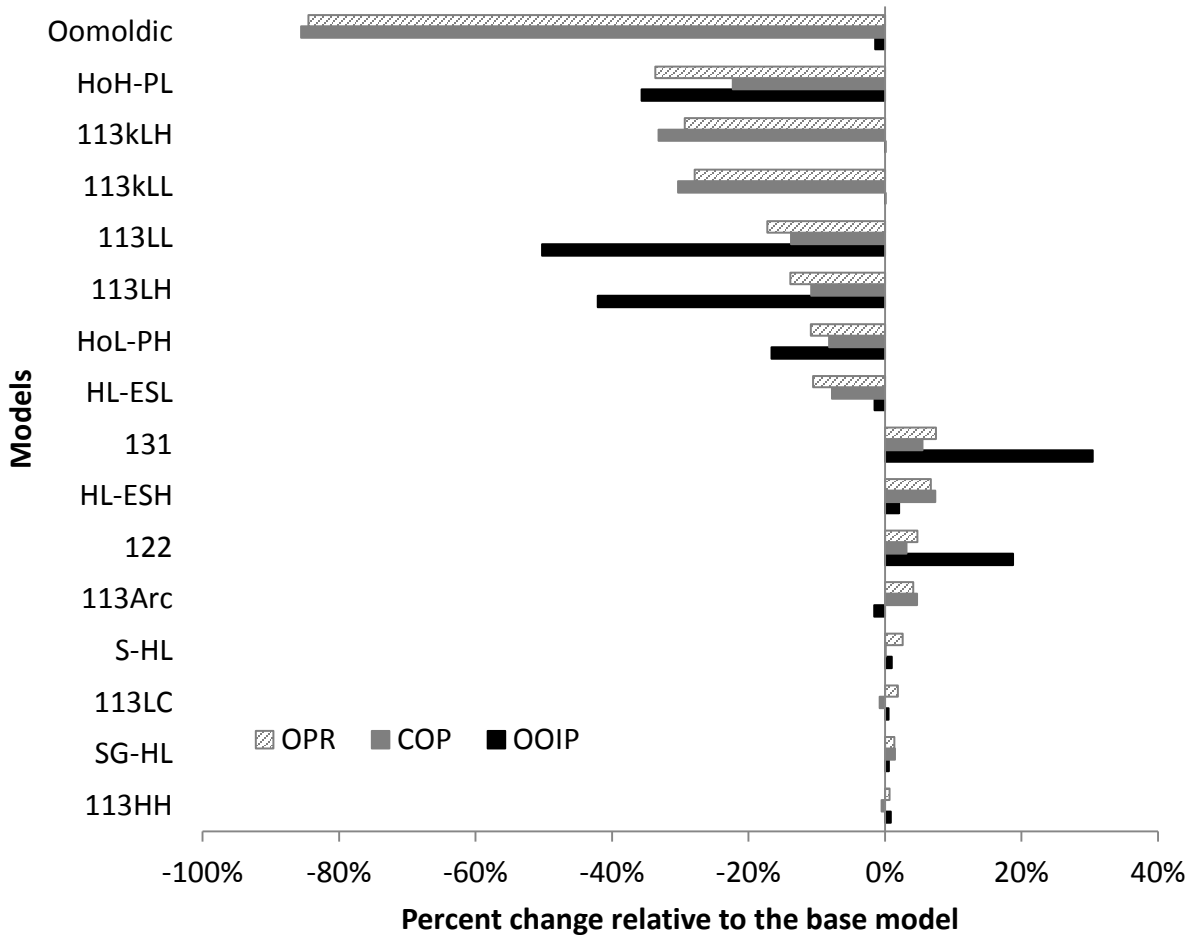

Figure 10. Plot of change in OOIP, production rate, and cumulative production relative to the base model for all models, ranked by changes in production rate (largest at top, smallest at the base). OPR = Oil production rate, COP = Cumulative oil production; OOIP = Original oil in place. Note that the geological changes can increase or decrease production metrics to various extents. See text for the geological meaning of the various models and discussion.

Facies	Texture	Grain Size	Grain Type	Sedimentary Structures	Interpretation
A	Framestone-Boundstone	medium-cobble	Corals, Skeletal (matrix)	*in situ* corals	Reef
B	Grainstone	fine-medium	Ooids, Peloids, Skeletal	extensive bioturbation	Lower Shoreface
C	Grainstone	medium-coarse	Ooids, Peloids, Skeletal	trough-cross stratification	Upper Shoreface
D	Grainstone	fine-coarse	Ooids, Skeletal	low angle (2-11°); planar, coarse-fine laminations; fenestrae; rhizoliths; interclasts	Foreshore
E	Grainstone	fine-coarse	Ooids, Skeletal	rhizoliths, laminated crust, karst features	Subaerial exposure surface

Table 1. Summary of facies attributes of outcrop exposures from Long Cay.

Heterogeneity	Settings		
1) Depositional geometry	Clinoform 	Layer Cake 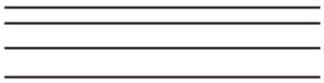	
2) Plan-view ridge pattern	Strike Parallel 	Arcuate 	
3) Vertical facies proportion	1:1:3 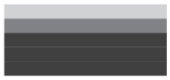	1:2:2 	1:3:1 
4) Flow barriers between ridge sets	Absent 	Present 	

Table 2. Simple representations of the stratigraphic and sedimentologic heterogeneities captured through the suite of models. Graphics are for illustration only; no absolute scale is implied.

	Model	Facies	Values	Variability	Mean	Standard Deviation
Porosity	113LL	C/D	Low	Low	10	1
		B	Low	Low	5	1
	113LH	C/D	Low	High	10	5
		B	Low	High	5	5
	113HL	C/D	High	Low	20	1
		B	High	Low	10	1
	113HH	C/D	High	High	20	5
		B	High	High	10	5
Permeability	113kLL	C/D	Low	Low	200	100
		B	Low	Low	100	50
	113kLH	C/D	Low	High	200	400
		B	Low	High	100	200

Table 3. Summary table of parameters for models varying porosity or permeability.

Black oil model	
Property	
Oil density (kg/m^3)	801
Oil Gravity (API)	45
Formation volume factor (m^3/Sm^3)	1.01
Initial pressure (bar)	136
Bubble point pressure (bar)	300
Vertical permeability ratio	0.1
Gas-oil contact (m)	1375
Oil-water contact (m)	1450

Table 4. Summary of engineering parameters held constant for all flow simulations.

APPENDIX

113HL (Base)	Clinoform geometry, 1:1:3 facies proportions (foreshore, upper shoreface, lower shoreface), high porosity values with low variance (see porosity matrix for values). Permeability is 200 md (horizontal [I,J]) and 20 md (vertical [K]). Net/Gross = 1
113LL	Low porosity values with low variance (see porosity matrix for values)
113LH	Low porosity values with high variance (see porosity matrix for values)
113HH	High porosity values with high variance (see porosity matrix for values)
122	1:2:2 facies proportions
131	1:3:1 facies proportions
113LC	Layer-cake' geometry
S-HL	Layer-cake' geometry with stochastically distributed 1:1:3 facies proportions
SG-HL	Stochastically distributed 1:1:3 facies proportions
Oomoldic	Permeability is 20 md (horizontal [I,J]) and 2 md (vertical [K])
HL-ESH	Clinoforms are bounded by exposure surfaces (30% phi and 1 D k) acting as fluid flow conduits
HL-ESL	Clinoforms are bounded by exposure surfaces (0 phi, 0 k) acting as fluid flow barriers
HoH-PL	Clinoform bounding exposure surfaces (0 phi, 0 k), Holocene (seaward) clinoforms have high porosity values with low variance while Pleistocene (landward) clinoforms have low porosity values with low variance (see porosity matrix for values)
HoL-PH	Clinoform bounding exposure surfaces (0 phi, 0 k), Holocene clinoforms have low porosity values with low variance while Pleistocene clinoforms have high porosity values with low variance (see porosity matrix for values)
113kLL	Low permeability values with low variance (see permeability matrix for values). Porosity is 10% for all facies
113kLH	Low permeability values with high variance (see permeability matrix for values). Porosity is 10% for all facies
113Arc	Uses an arcuate ridge set morphology (See Figure 3)

Table A1. Model nomenclature explanation. All models follow Base model (113HL) parameters unless otherwise stated in explanation.